An Application of 3-D Hydrodynamic Model in a Very Shallow Lagoon

A. Pollani[1] , **G. Karantounias**[2]

1. Hellenic Centre for Marine Research, Institute of Oceanography,
P.O.Box 712, Anavissos, Attica, Greece
2. Laboratory of Agricultural Hydraulics, Agricultural University of Athens,
Iera Odos 75, 11855 Athens, Greece

Abstract

In this paper objectively analyzed data as well as simulated results are presented for the area of the Kotychi lagoon. A 3-D hydrodynamic model was used to describe the velocity, temperature and salinity fields. Simulation results are in good agreement with the observed data illustrating the role of the atmospheric forcing in determining the variability of the circulation.

1. Introduction

Kotychi is the largest and most significant lagoon in Peloponnisos. The lagoon is of great ecological and economic interest and is protected by the Ramsar International Convention. It is a very shallow lagoon with a depth of 30 to 40 cm which receives considerable freshwater inputs from the adjacent streams causing significant seasonal salinity fluctuations. The water depth is reduced by the deposition of suspended matter brought into the lagoon by these streams. The lagoon is considered eutrophic to hypertrophic. At the centre of its western side there is an opening almost 30m in width linking the lagoon to the Ionian Sea. On the bottom of the lagoon channels of 1m depth were constructed converging in front of the opening where is the deepest area of the lagoon (approx. 5m deep). This human intervention contributes to the circulation of the water masses and the renewal of the lagoon water. The climate is generally mild with an average annual precipitation of 833 mm and an average annual temperature of 16 ^{o}C. The coldest month is December (approx. 10 ^{o}C) and the hottest is August (approx. 25 ^{o}C).

2. Objective analysis

According to this method data fields are calculated from individual observations on a grid of sampling stations. The scheme used in this study is similar to that described by

Levitus (1982) which is an interactive difference-correction scheme (Cressman, 1959) with a weight function developed by Barnes (1964). First the area is divided into equally spaced boxes (grid), which in this case were 30m and the first guess *F* is determined by setting the initial value of the analysis grid to the arithmetic average of the observations in the area. Then the difference between the raw observed data *R* and the first guess *F* is computed:

$$Q_{ij} = R_{ij} - F_{ij} \tag{1}$$

at grid point i,j
Following the smoothed analysis increments are calculated:

$$C_{ij} = \frac{\sum_{s=1}^{n} W_s Q_s}{\sum_{s=1}^{n} W_s} \tag{2}$$

where W_s is the Barnes weight function: $W_s = \exp(-4r^2R^{-2})$ for $r \le R$ where r is the distance between the S^{th} data point and the grid point (i,j) and R the radius influence.

Once the smoothed analysis increments have been computed they are used to update the first guess:

$$F_{ij} = F_{ij} + C_{ij} \tag{3}$$

Finally a 5-point linear filter (Shapiro, 1970) was used according to which the smoothed value at a grid point is:

$$S_{ij} = G_{ij} + \frac{a}{4}(G_{i-1,j} + G_{i+1,j} + G_{i,j-1} + G_{i,j+1} - G_{i,j}) \tag{4}$$

where a is a smoothing parameter. Two passes with the filter are suggested with a=0.5 for the first pass and a=–0.5 for the second pass. Since the amplitude of the large scales may be dumped in the first pass it is restored with the second pass. The filter is not applied to grid points located on the land as well as if any of four adjacent grid points is located over land.

The above sequence was repeated with a different radius of influence *R* that decreased with each pass. The reason for this is that large *R* makes small corrections in the large gaps between stations while with smaller values more spatial resolution is retained in regions with densely spaced stations. Four passes were performed in total with radii of influence of 240, 150, 120, 90 and 60 m respectively.

3. The modelling system

The modeling system is the Princeton Ocean Model (POM), a free surface primitive equation general circulation model using curvilinear orthogonal horizontal coordinates and a sigma layers system in the vertical. It uses two sub-models for the computation of the eddy mixing (second order turbulence closure scheme) and horizontal non-linear viscosity. It also uses a time splitting technique for the external (barotropic) and internal (baroclinic) modes. POM has been extensively described in the literature (Oey, 1985a,b, Blumberg and Mellor 1987, Galperin and Mellor 1990, Mellor and Ezer, 1991) and is accompanied by a comprehensive User's guide (Mellor and Ezer, 1991). It has been successfully applied in a variety of systems from Lagoons (Petihakis et al., 2000) to coastal and enclosed areas (Petihakis et al. 2001, Petihakis et al. 2002, Triantafyllou et al. 2003, Triantafyllou et al. 2003) and to offshore deep systems (Petihakis, et al. 2002, Triantafyllou et al., 2003) to list some of them.

Potential temperature, salinity, velocity and surface elevation, are prognostic variables of the model. It solves the following equations for the ocean velocity U_i = (U,V,W), potential temperature T and salinity S:

$$\frac{\partial U_i}{\partial x_i} = 0 \tag{5}$$

$$\begin{aligned} &\frac{\partial}{\partial t}(U,V) + \frac{\partial}{\partial x_i}\left[U_i(U,V)\right] + f(-V,U) = \\ &= -\frac{1}{\rho_o}\left[\frac{\partial p}{\partial x},\frac{\partial p}{\partial y}\right] + \frac{\partial}{\partial z}\left[K_M \frac{\partial}{\partial z}(U,V)\right] + (F_U,F_V) \end{aligned} \tag{6}$$

$$\frac{\partial T}{\partial t} + \frac{\partial}{\partial x_i}\left[U_i T\right] = \frac{\partial}{\partial z}\left[K_H \frac{\partial T}{\partial z}\right] + \frac{\partial R}{\partial z} + F_T + \frac{1}{r(z)}(T_{CLIM} - T) \tag{7}$$

$$\frac{\partial S}{\partial t} + \frac{\partial}{\partial x_i}\left[U_i S\right] = \frac{\partial}{\partial z}\left[K_H \frac{\partial S}{\partial z}\right] + F_S + \frac{1}{r(z)}(S_{CLIM} - S) \tag{8}$$

The hydrostatic approximation yields:

$$\frac{p}{\rho_o} = g(n - z) + \int_z^n \frac{\rho - \rho_o}{\rho_o} g\,dz \tag{9}$$

where n is the free surface elevation, ρ_o is a reference density and

$\rho = \rho(T, S, p)$ is the density calculated by an adaptation of the UNESCO equation of state by Mellor (1991).

The horizontal diffusion terms (F_U, F_V), F_T and F_S in (6), (7) and (8) are evaluated using the Smagorinsky (1963) horizontal diffusion formulation. The fourth term on the r.h.s of equations (7) and (8) represents a depth-dependent nudging towards the climatology.

The vertical mixing coefficients K_M and K_H in equations (6) - (8) are computed according to the Mellor-Yamada 2.5 turbulence closure scheme (Mellor and Yamada, 1982). Finally, the term *R* in (7) is the portion of the net shortwave radiation flux that penetrates the sea surface.

4. The model grid, bathymetry and initial conditions

The model is implemented in the geographical area that lies between 37.99° to 38.025° N and 21.275° to 21.317° E.

The horizontal grid contains 31×67 computational grid points. The model uses a bottom-following, sigma coordinate system. It has 7 sigma levels in the vertical which follow a logarithmic distribution near the surface in order to correctly resolve the dynamics of the surface mixed layer.

The model's bathymetry was obtained from coarse bathymetric maps by bilinear interpolation. A Shapiro filter (1970) of third order was also applied to the interpolated bathymetry in order to perform the necessary smoothing (elimination of small scale noise). Figure 1 shows the bathymetry of the computational domain (cm).

The model's run was initialized with January surface temperature and salinity fields. These data were mapped on the model's horizontal grid using bilinear interpolation and the surface values were extrapolated to all sigma layers. Additionally, initial velocities were set to zero.

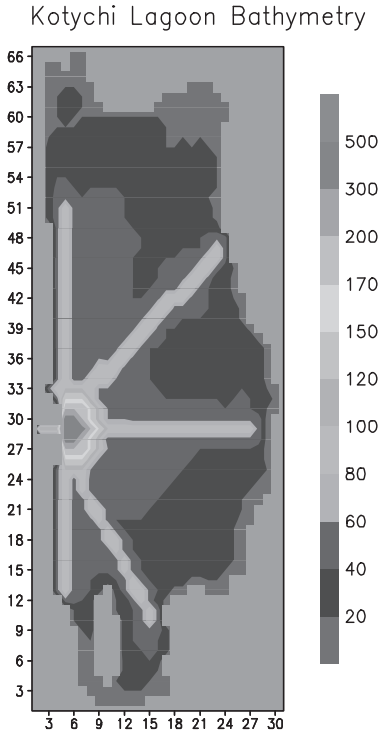

Figure 1. The Kotychi lagoon computational domain and its bathymetry (in cm).

5. Results and conclusions

Objectively analysed results

From the objectively analysed data (figures 2 and 3) there is an obvious influence in the lagoon waters from the two irrigation channels as well as by the sea. Water temperatures are higher at the inner part of the lagoon (15.8-16.4ºC during winter and 25.2-25.35ºC during summer), away from the communication point with the open sea which provides cooler water (14.2-15.4ºC during winter and 25.0-25.15ºC during summer). An interesting feature is that the water enters the lagoon rather than the lagoon waters outflow into the sea, as indicated by the temperature differences.

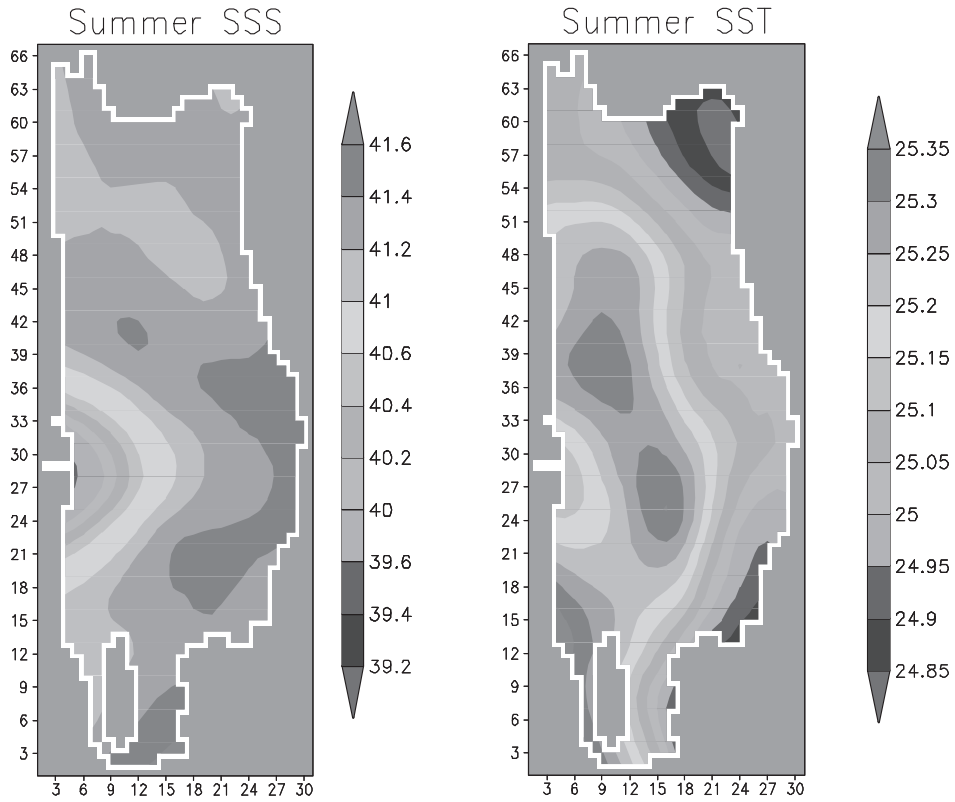

Figure 2. Sea Surface Salinity and Sea Surface Temperature for the summer period.

Salinity distribution shows high values, as expected in very shallow water bodies, especially during summer. Lower values are shown in the area close to the irrigation

channels during the winter time (29-32 psu) and in the area close to the opening connecting the lagoon with the sea during the summer time (39.2-40.6 psu). Note that the gradients in front of the opening (in both figures 2 and 3) are not well represented due to the sparse observations in this area.

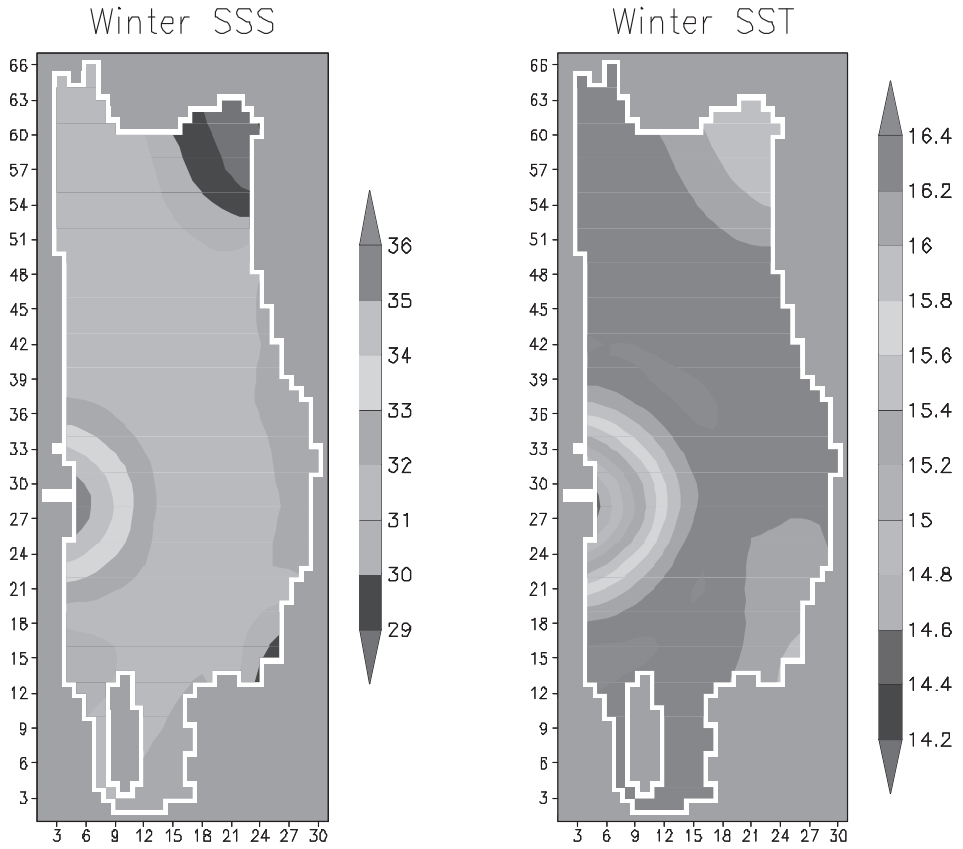

Figure 3. Sea Surface Salinity and Sea Surface Temperature for the winter period.

Simulation results

The circulation field is shown in figure 4 for the winter period. Cyclones and anticyclones are a characteristic feature strongly related to the channels' existence (human intervention). The velocities exhibit high spatial variability that might be attributed to the bottom topography developing a sequence of cyclones and anticyclones. There is a major anticyclone covering almost the north part of the basin, exhibiting increased velocities in the north-eastern part of the lagoon.

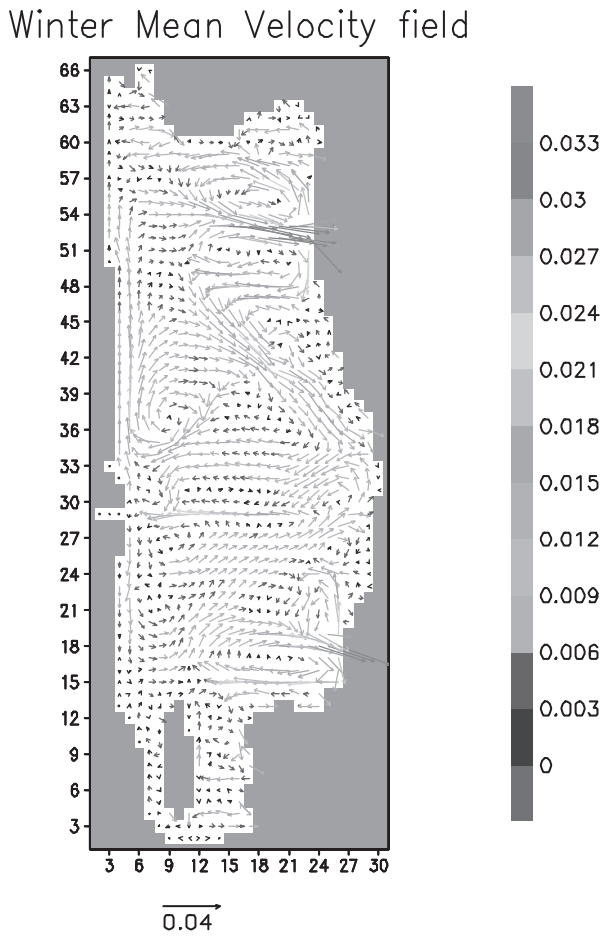

Figure 4. Simulation results: Winter mean velocity field.

Figure 5 shows model results for winter temperature and salinity. Temperature ranges approximately from 15 to 16ºC. Increased values are observed in the south part of the basin and in the north part where a characteristic tongue is developed by the major anticyclone existing there. The combination of those water masses of increased temperature values squeeze the colder water coming from the open boundary in a small area a little souther of the opening. Additionally the entrance of the fresh riverine water is nicely depicted in the north-eastern part of the lagoon.

Salinity concentrations of about 37.9 psu cover most of the basin with the exceptions of the north-eastern and the south-eastern parts where river fresh water inputs are shown, exhibiting strong gradients in those areas.

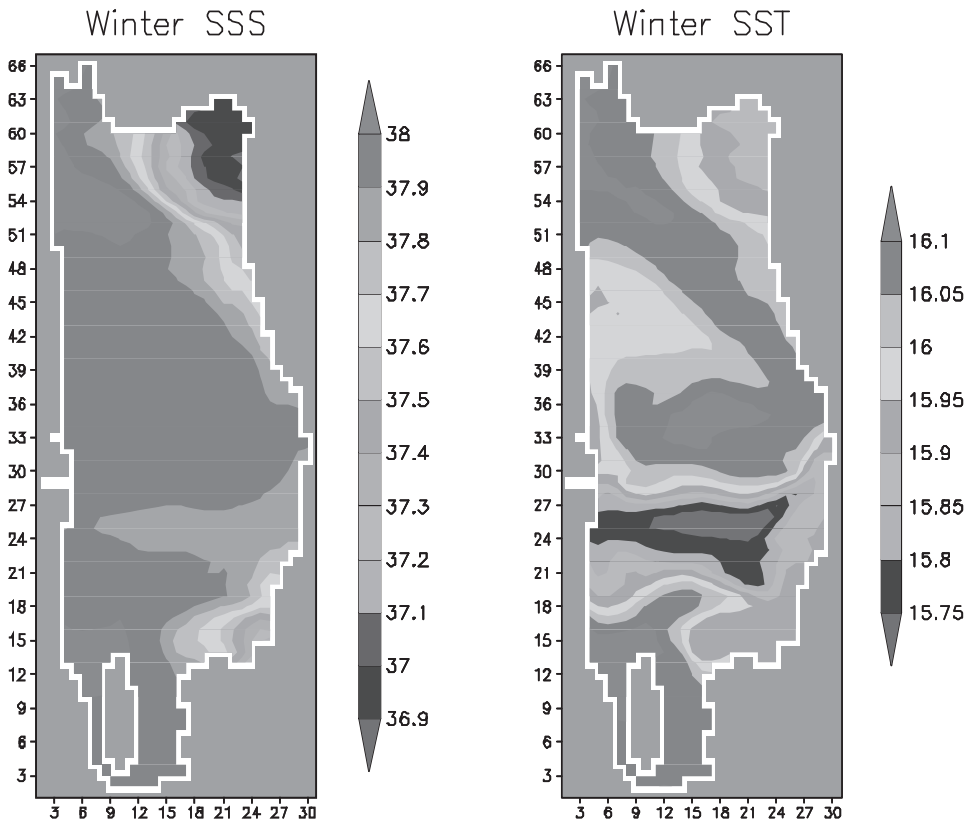

Figure 5. Simulation results: Winter Sea Surface Salinity and Sea Surface Temperature.

6. Conclusions

In this work we have presented the implementation of the POM on the Kotychi lagoon. The runs of the model have shown significant variability within the lagoon with strong flow patterns and intense horizontal gradients, as it was expected due to lagoon's shallowness.

Overall, the model in its basic run is characterized by a fairly good skill in reproducing basic circulation features of the lagoon. However due to the sparseness of the available observational data within the lagoon basin, several aspects of the general circulation cannot be evaluated. To this end, a continuous monitoring program would help to better understand the physical processes and would offer new insights to the Kotychi lagoon seasonal variability.

Furthermore, it should be interesting to couple an ecological model with the existing hydrodynamic one for the investigation of the ecosystem functioning. This work is in progress and will be published elsewhere.

References

1. Barnes, S. L., 1964. A technique for maximizing details in numerical weather map analysis. Journal of Applied Meteorology, 3: 396-409.
2. Blumberg, A. F. and Mellor, G. L., 1987. A description of a three-dimensional coastal ocean circulation model. Three-Dimensional Coastal Ocean Circulation Models. N. S. Heaps. Washington, D.C., AGU., 4: 1-16.
3. Cressman, G. P., 1959. An operational objective analysis scheme. Mon. Weather Rev., 87: 329-340.
4. Galperin, B. and Mellor, G. L., 1990. A time-dependent, three-dimensional model of the Delaware Bay and River. Part 2: Three-dimensional flow fields and residual circulation. Estuarine Coastal and Shelf Science, 31: 255-281.
5. Galperin, B. and Mellor, G. L., 1990. A time-dependent, three-dimensional model of the Delaware Bay and River. Part I: Description of the model and tidal analysis. Estuarine Coastal and Shelf Science, 31: 231-253.
6. Levitus, S., 1982. Climatological Atlas of the World Ocean. Washington, NOAA: 173.
7. Mellor, G. L., 1991. An equation of state for numerical models of oceans and estuaries. Journal Atmospheric Oceanic Technology, 8: 609-611.
8. Mellor, G. L. and Ezer, T., 1991. A Gulf Stream model and an altimetry assimilation scheme. Journal of Geophysical Research, 96: 8779-8795.
9. Oey, L. Y., G. Mellor, L. , et al., 1985a. A three-dimensional simulation of the Hudson-Raritan estuary. Part I: Description of the model and model simulations. Journal of Physical Oceanography, 15: 1676-1692.
10. Oey, L. Y., G. Mellor, L. et al., 1985b. A three-dimensional simulation of the Hudson-Raritan estuary. Part II: Comparison with observation. Journal of Physical Oceanography, 15: 1693-1709.
11. Petihakis, G., Triantafyllou, G. et al., 2002a. Modelling the Spatial and Temporal Variability of the Cretan Sea Ecosystem. Journal of Marine Systems, 36: 173-196.
12. Petihakis, G., Triantafyllou, G. et al., 2002b. Exploring the dynamics of a marine ecosystem (Pagasitikos Gulf, Western Aegean, Greece) through the analysis of temporal and spatial variability of nutrients. The Changing Coast. V. Gomes, T. Pinto and L. das Neves. Porto, EUROCOAST. 2: 513-522.
13. Petihakis, G., Triantafyllou, G. et al., 2001. Prediction and prevention of oil contamination and monitoring of the benthic structure and related fisheries in connection with the pollution impact. Systems Analysis Modelling Simulation, 41(1): 169-197.

443

14. Petihakis, G., Triantafyllou, G. et al., 2000. Modelling the annual cycles of nutrients and phytoplankton in a Mediterranean lagoon (Gialova Greece). Marine Environmental Research, 48(1): 37-58.
15. Shapiro, R., 1970. Smoothing, filtering, and boundary effects. Reviews of Geophysics and Space Physics, 8(2): 359-387.
16. Smagorinsky, J., 1963. General circulation experiments with the primitive equations, I, The basic experiment. Mon. Weather Rev., 91: 99-164.
17. Triantafyllou, G., Hoteit, I. et al., 2003. A singular evolutive interpolated Kalman filter for efficient data assimilation in a 3D complex physical-biogeochemical model of the Cretan Sea. Journal of Marine Systems, 40-41: 213-231.
18. Triantafyllou, G., Korres, G. et al., 2003a. Assessing the phenomenology of the Cretan Sea shelf area using coupling modelling techniques. Annales Geophysicae, 21: 237-250.
19. Triantafyllou, G., Petihakis, G. et al., 2003b. Assessing the performance of the Cretan Sea ecosystem model with the use of high frequency M3A buoy data set. Annales Geophysicae, 21: 365-375.